

Quantitative Model of the Formation Mechanism of the Rollfront Uranium Deposits

D.Y. Aizhulov^{1*}, N.M. Shayakhmetov¹, A. Kaltayev²

¹Al-Farabi Kazakh National University, 71 al-Farabi Ave., Almaty, Kazakhstan, 050040

²Satbayev University, 22a Satpayev street, Almaty, Kazakhstan, 050013

Article info

Received:
16 February

Received in revised form:
18 April 2018

Accepted:
27 June 2018

Abstract

The rollfront type deposits are crescent shaped accumulation of mineralization including uranium, selenium, molybdenum in reduced permeable sandstones. It generally forms within a geochemical barrier between mostly reduced and predominantly oxidized environments. Redox reactions between oxidant and reductant creates favorable conditions for uranium precipitation, while constant flow of oxidant continuously dissolves uranium minerals thereby creating a reactive transport. Several previous works had either focused on the characteristics of the rollfront type deposits, or on the description of chemical and geological processes involved in their genesis. Based on these previous works, authors aimed to mimic laboratory experiments numerically by reactive flow and numerical simulation. Data from one particular experiment was used to determine reaction rates between reactants to produce a model of reactive transport and chemical processes involved in the formation of rollfront type deposits. The resulting model was used to identify the causes of crescent like formations and to determine main mechanisms influencing rollfront evolution. A better understanding and simulation of the mechanism involved in the formation of rollfront type deposits and their properties would contribute to decreased exploration and production costs of commodities trapped within such accumulations. The results of this work can be used to model other deposits formed through infiltration and subsequent precipitation of various minerals at the redox interface.

Nomenclature

C_{dis} – dissolved mineral concentration ($\text{g}\cdot\text{l}^{-1}$);
 C_{sol} – solid (precipitated) mineral concentration ($\text{g}\cdot\text{l}^{-1}$);
 C_{red} – reduced environment concentration ($\text{g}\cdot\text{l}^{-1}$);
 C_{ox} – oxidizer concentration ($\text{g}\cdot\text{l}^{-1}$);
 C_e – electron bearing elements concentration ($\text{g}\cdot\text{l}^{-1}$);
 C_{pr} – product of reductant oxidation concentration ($\text{g}\cdot\text{l}^{-1}$);
 $k_i, i = \overline{1,4}$ – reaction constant for each reaction;
 ρ – total density ($\text{kg}\cdot\text{m}^{-3}$);
 ρ_{liquid} – liquids density ($\text{kg}\cdot\text{m}^{-3}$);
 ρ_{solid} – solids density ($\text{kg}\cdot\text{m}^{-3}$);
 K – permeability (m^2);
 $\vec{u} = \{u_x, u_y\}$ – flow velocity ($\text{m}\cdot\text{sec}^{-1}$) with its components by x and y axes;
 μ – viscosity ($\text{Pa}\cdot\text{sec}$);
 p – pressure (Pa);
 t – time (sec);
 θ – porosity.

1. Introduction

Adams and Cramer [1] define rollfront uranium deposits as a build-up of a mineral resource such as uranium (U), selenium (Se), and molybdenum (Mo) in reduced permeable sediments (mostly sandstones) along the border (the border being the rollfront) between prevalently reduced and pervasively oxidized environments. In terms of geometry, the International Atomic Energy Agency gives the following definition for rollfront deposits: “zones of uranium-matrix impregnations that crosscut sandstone bedding and extend vertically between overlying and underlying less-permeable horizons” [2]. Dahlkamp [3] defines the following properties for the rollfront deposits: they have elongate and sinuous shape in aerial view with lines being perpendicular to the direction of the groundwater flow; mineralization zones are convex down vertically;

*Corresponding author. E-mail: daniar.aizhulov@gmail.com

they have diffuse boundaries with reduced sandstone on the downstream side of the groundwater flow and sharp contacts with oxidized sandstone on the upstream of groundwater flow side. Rollfront is a sedimentary and epigenetic (occurred after hosting environment was created) mineral deposit, that occurs in dry areas and trapped within permeable environments.

Rollfronts are undeniably important types of deposits for the mining industry, and in particular for uranium sphere. Rollfront type uranium deposits account for as much as 60% of the worldwide production [4] compared to the other recoverable uranium resources in sandstone environments. Principal uraniumiferous sandstone provinces include the Colorado Plateau, Wyoming, Texas Coastal Plain, Mali-Nigeria, Czech Cretaceous Plate, Chu-Sarysu, Syr-Daria, and Kyzylkum in Kazakhstan [5]. The publication on the World Uranium Deposits by the International Atomic Energy Agency [2] mentions the following rollfront type deposits: Moynkum, Inkai and Mynkuduk (Kazakhstan), Crow Butte and Smith Ranch (USA) and Bukinay, Sugraly and Uchkuduk (Uzbekistan). Kazakhstan is the second largest country in the World by its amount of uranium resources close to a million tons of recoverable uranium (1Mt U in 2013), almost 70% of which can be recovered using In-Situ Leaching (ISL) method [4]. Better understanding of reactive transport and chemical mechanisms involved in the formation of rollfront deposits would help in performing safe and cost-effective ISL for exploiting these kind of deposits.

One of the main difficulties in the exploration of uranium rollfront type deposits lies in the limited number of available exploration techniques that, at small scale, are generally limited to the drilling of costly systematic numerous well network patterns in perspective areas. A better knowledge of the spatial distribution of uranium mineralized zones can optimize the production in operational mines. Numerous stochastic techniques for modeling rollfronts were investigated by Renard D., Beucher H. [6], Petit et al. [7] and Abzalov et al. [8]. However, they rarely account for the hydrodynamic and chemical processes involved in the deposit genesis that hence could enhance these existing techniques.

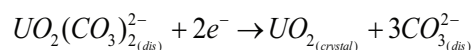
This work intends to numerically reproduce empirical experiment results on rollfront formation process, and to develop appropriate quantitative model of the formation mechanism of the rollfront that can be applied for various bedded geometries.

The genesis of rollfront type deposits comprises three main stages (Fig. 1): leaching phase by

oxygenated water, migration of the diluted chemical components and lastly deposition of minerals. In the case of the Tianshan mega-province, southern Kazakhstan, which hosts as much as 1.400 Mt of uranium [5], oxygen rich rainwater leached uranium-enriched minerals including zircons, monazites, and accessory minerals, from the granitic Tianshan Mountains, and then transported it downstream through the unconsolidated porous sandstones. Later on, when reaching reduced environments, the dissolved uranium together with other elements such as iron and sulfurs precipitated as uranium minerals (mainly pitchblende and coffinite in the Kazakhstan uranium deposits) and pyrite (FeS_2), thereby forming a rollfront type deposit. It is important to note, that the re-deposition of minerals is a dynamic dissolving/precipitation process sustained by a continuous flow of oxygenated meteoritic water which push minerals further downstream. In other words, in active deposits, minerals continuously dissolve from the upstream side of the mineralization zone and precipitate at the front side rear. When no more oxygen is available in the water flow, often because it has been consummated previously by the oxidation of the organic matter before reaching the mineralized zone, the rollfront stabilize.

Evidently, uranium precipitation/dissolution can involve complicated chemical complexes. The lack of knowledge of exact chemicals compounds involved in the reactive transport process, leads to a challenging problem for modeling rollfront deposits formation. In addition, temperature, pressure, Eh and pH are factors that affect uranium precipitation. Low oxidation and high pH both contribute to precipitated minerals [10].

There are many uranyl and uranous complexes that can form with various anions, including sulfates (UO_2SO_4 , USO_4^{2+}), carbonates ($\text{UO}_2(\text{CO}_3)_2^{2-}$, UO_2CO_3), phosphates (UO_2HPO_4 , $\text{UO}_2(\text{HPO}_4)_2^{2-}$), chlorides (UCl^{3+} , UO_2Cl^+) or fluorides (UO_2F^+ , UF^{3+}). Assuming that, uranium migrates in oxygenated aquifers mostly as carbonate anions ($\text{UO}_2(\text{CO}_3)_3^{4-}$, or $\text{UO}_2(\text{CO}_3)_2^{2-}$) [11], the general scheme for uranium precipitation upon reaching reduced environment can be written as follows [11]:



Reduced environment such as pyrite and organic matters provides the necessary electrons in order to precipitate the uranium.

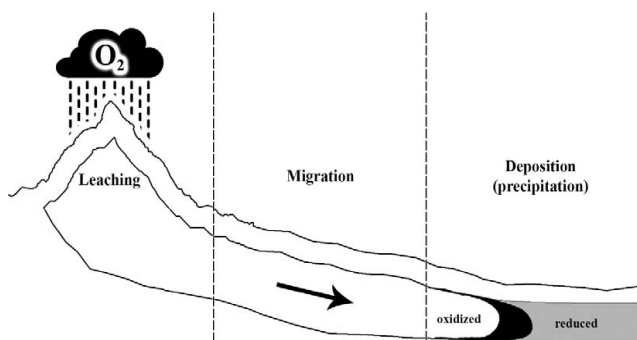
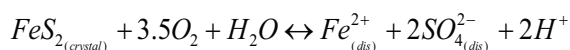
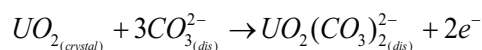


Fig. 1. Schematic stages for the formation of rollfront deposit.

Oxygenated waters interact with reduced environment, thereby forming a geochemical barrier that creates favorable conditions for uranium precipitation. For instance, pyrite can supply electrons to the medium by oxidizing the iron that changes from the oxidation state ferrous Fe^{2+} to ferric Fe^{+3} releasing sulfate ion SO_4^{2-} in the water:



Oxygenated waters turn precipitated uranium minerals back into dissolved form. Dissolution reaction of crystalized uranyl dioxide back into uranyl carbonate can be described by the following chemical half-reaction:



Evseeva et al. [12] conducted a dissolution/precipitation experiment in which she managed to mimic the formation of the uranium rollfront deposits in laboratory conditions. The experimental results were compared with the numerical results of the model by reproducing the experiment conditions. Evseeva used a transparent plastic box ($2 \times 0.15 \times 0.2$ m) filled with sand. After several chemical manipulations, the iron oxide contained in the box was converted to sulfides thereby creating a reduced environment. A water containing uranium concentration (around 10^{-6} – 10^{-5} g·l⁻¹ gram per liter) was flowed through the box leading to the formation of a roll-like accumulation of uranium in the box.

The resulting distribution of the uranium in the box is due to a stable increase in uranium concentration and the shifting of the oxidation zone into the reduced sands. When the experiment was conducted, showing that the above-mentioned laboratory experiment reproduces quite well the roll-like accumulations of uranium, there was no

satisfactory explanations on the mechanisms responsible for the occurrence of such shapes.

Since rollfront deposits form in porous medium, as underlined by Goldshtik M.A. [9], a definitive diffusive extension of a deposit “tongue” (or uranium wings) cannot be explained by not considering a slip boundary conditions for the viscous flow. Other factors must be responsible for the formation of the crescent shaped mineralization.

Rollfront accumulations were formed due to the interaction between oxidizer and reducer. However, there was no noticeable re-deposition of uranium, probably due to the low oxidizer concentrations and/or insufficient time to dissolve and mobilize uranium. In other words, the uranium concentrations were higher at the beginning of the box, and gradually decreased along its length.

Based on the analysis of existing data the aims of this work were to identify the causes of crescent like formations and to determine main mechanisms influencing rollfront evolution.

2. Numerical experiments

The medium under consideration is porous and permeable, while the Darcy equation is a time-tested instrument to simulate underground fluid flow in porous medium [13]:

$$\text{div}(\rho_{liquid}\phi\vec{u}) + \frac{\partial(\phi\rho_{liquid})}{\partial t} = 0 \quad \phi\vec{u} = -\frac{K}{\mu} \text{grad } p$$

where the first equation describes the mass conservation, whereas the second one defines the flow velocity in the porous medium. Several components, both dissolved and solids, migrate and react inside the porous media. In accordance with Fick’s Law, for each component i mass conservation equation can be rewritten in following form:

$$[\text{div}(\phi\rho_i\vec{u}) - \text{div}(\phi D_i \text{grad}\rho_i)] + \frac{\partial(\phi\rho_i)}{\partial t} = 0$$

where ρ_i are densities and D_i are diffusive coefficients of each component i .

Taking into account reactions between components, the general concentration equation for each component i can be described by the following equation:

$$\text{div}(\phi\rho_i\vec{u}) - \text{div}(\phi D_i \text{grad}\rho_i) + \frac{\partial(\phi\rho_i)}{\partial t} = W_i$$

where W_i is a chemical term. Same formula can be rewritten for concentrations as

$$\frac{\partial(\phi c_i)}{\partial t} + \text{div}(\phi c_i \vec{u}) - \text{div}(\phi D_i \text{grad} c_i) = w_i$$

while reaction rate [$\text{mol} \cdot \text{L}^{-1} \cdot \text{s}^{-1}$] and molar density (or molar concentration) [mol/L] c_i are equal to $w_i = W_i/M_i$ and $c_i = \rho_i/M_i$ respectively.

The Gulberg-Waage's Law of Mass Action is used to describe the equilibrium of the various chemical species [14]. The reaction rate depends on: the concentration of reactants involved: the probability of occurrences of the reaction due to the collision between species, and to the time required for a specific chemical reaction to take place. For example the reaction rate between two reagents A and B would be equal to $w_i = k C_A C_B$ with k being the temperature-pressure-dependent chemical reaction constant, and $C_A C_B$ being the concentration (proportional to the collision probability of particles).

Several assumptions were made in the context of the experiment:

- the fluids in the box are incompressible, and the flow of reagents occur in the water;
- the diffusive transport of the mineral is much lower in comparison with convective transport;
- the amount of reductant is much higher than of other reagents;
- temperature is constant;
- porosity does not change through time;
- the concentration of oxidant used in the experiment were as low as $0.001 \text{ g} \cdot \text{l}^{-1}$ which would be close to the groundwater oxygen concentrations in Central Asia deposits [11].

To reproduce Evseeva's laboratory experiment a 2D box was considered as a domain for numerical calculations, with inlet on the left and outlet on the right (Fig. 2).

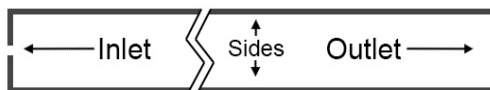
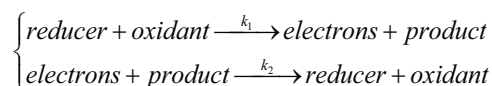


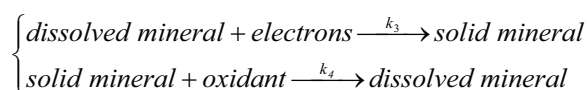
Fig. 2. Schematic representation of the domain for numerical calculations.

Based on the aforementioned principles of roll-front formation and laboratory experiment following scenario was simulated by numerical experiment. Into the box containing porous medium with high concentration of a reductant C_{red} , a constant inflow of water with concentrations of dissolved uranium C_{dis} and oxidant C_{ox} was imposed through inlet over a period of 60 days. Redox reaction between reductant and oxidant are simplified by the following scheme:



where electron bearing elements concentration C_e and additional product concentration C_{pr} are a result of reductant oxidation.

Electron bearing elements contribute to the dissolved uranium precipitation into a solid form, with dissolved uranium concentration C_{dis} and solid uranium concentration C_{sol} being involved in the model. As already mentioned, in the real world conditions, oxygenated waters redeposit minerals by dissolving them back to mobile complexes. Therefore, precipitation and dissolution of uranium minerals can be described by the following simplified scheme:



According to the Law of Mass Action [14], change in reductant concentration can be described by the equation

$$\frac{\partial C_{red}}{\partial t} = \frac{k_2 C_e C_{pr} - k_1 C_{red} C_{ox}}{(1-\phi)\rho_{solid}}$$

i.e. the decrease in reducer concentration is proportional to the amount of oxidant inflow and inversely proportional to the amount of redox products. Reductant is in solid phase and cannot be transported by convective flow, hence the absence of convective term. Similarly, the concentration of oxidant is spent on oxidizing solid uranium complexes as well as enclosing reductant and can be described by the following equation

$$\frac{\partial C_{ox}}{\partial t} + \vec{u} \cdot \text{grad} C_{ox} = \frac{k_2 C_e C_{pr} - k_1 C_{red} C_{ox} - k_4 C_{sol} C_{ox}}{\phi \rho_{liquid}}$$

where $\vec{u} \cdot \text{grad} C_{ox}$ is a convective term, added due to oxidant being in liquid phase. Change in redox product C_{pr} and electron concentration C_e can be described by

$$\frac{\partial C_{pr}}{\partial t} + \vec{u} \cdot \text{grad} C_{pr} = \frac{k_1 C_{red} C_{ox} - k_2 C_e C_{pr}}{\phi \rho_{liquid}}$$

and

$$\frac{\partial C_e}{\partial t} + \vec{u} \cdot \text{grad} C_e = \frac{k_1 C_{red} C_{ox} - k_2 C_e C_{pr} - k_3 C_e C_{dis}}{\phi \rho_{liquid}}$$

respectively.

The concentration of electrons is the main factor involved in the dissolution of uranium can be described by following equation

$$\frac{\partial C_{dis}}{\partial t} + \vec{u} \cdot \text{grad } C_{dis} = \frac{k_4 C_{sol} C_{ox} - k_3 C_{dis} C_e}{\phi \rho_{liquid}}$$

while inflow of oxidant is a main factor influencing uranium crystallization is described as

$$\frac{\partial C_{sol}}{\partial t} = \frac{k_3 C_e C_{dis} - k_4 C_{sol} C_{ox}}{(1 - \phi) \rho_{solid}}$$

Boundary conditions used in numerical experiment were similar to those of the laboratory experiment. According to the experiment Evseeva et al. [12], atmospheric pressure boundary condition is imposed at the outlet

$$p|_{outlet} = P_{atm}$$

while a constant boundary condition is imposed to the flow velocity at $1.44 \cdot 10^{-4} \text{ m}\cdot\text{s}^{-1}$ at the inlet, which corresponds to

$$p|_{inlet} = P_{atm} + \rho gh$$

with h equal to 0.74 m. Apart from inlet and outlet no-flow boundary condition is imposed to all solid sides of the box

$$\vec{u} \cdot \vec{n}|_{sides} = 0 \quad \text{or} \quad \frac{\partial p}{\partial n}|_{sides} = 0$$

Other boundary conditions for all concentrations in liquid phase, conform to following boundary conditions (measured in gram per liter):

$$C_{dis}|_{inlet} = 7.5 \cdot 10^{-5}, C_{ox}|_{inlet} = 0.002, C_e|_{inlet} = 0, C_{pr}|_{inlet} = 0$$

$$\frac{\partial C_{dis}}{\partial n}|_{sides} = 0, \frac{\partial C_{ox}}{\partial n}|_{sides} = 0, \frac{\partial C_e}{\partial n}|_{sides} = 0, \frac{\partial C_{pr}}{\partial n}|_{sides} = 0$$

corresponding to the fact that only dissolved uranium is injected into the system.

The initial conditions for the concentrations of liquids are:

$$C_{dis}|_{t=0} = 0, C_{ox}|_{t=0} = 0, C_e|_{t=0} = 0, C_{pr}|_{t=0} = 0$$

The initial conditions for the concentrations of solids are:

$$C_{sol}|_{t=0} = 0, C_{red}|_{t=0} = 1$$

Before the inflow started, there was no uranium in the box, and it was filled with the reduced porous medium (sand + ferrous iron).

According to this model, the solid uranium can only form by a precipitation reaction only. An analytical solution to the set of the considered differential equations given the above boundary and initial conditions is quite difficult to achieve; thus they were solved numerically using the COMSOL Multiphysics software.

Additional parameters values used in the experiment are shown on the Table 1 below.

Table 1

Additional parameters values used in the experiment

Parameter	Value
Porosity (ϕ)	0.4
Permeability (K)	1 mD or $1\text{E-}15 \text{ m}^2$
Density of liquid (ρ^{liquid})	$1000 \text{ kg}\cdot\text{m}^{-3}$
Solids density	$1700 \text{ kg}\cdot\text{m}^{-3}$
Lengths of the chamber	2 m
Height of the chamber	0.125 m (excluding clay layers)

3. Results and discussions

After several trial-error adjustments of the reaction rates, results of the numerical simulation begin to conform with the experimental data (Fig. 3). The reason for the uranium concentrations being higher at the beginning of the box is most likely due to the slow oxidation rate (compared to flow velocity) of the uranium minerals. Although some of the solid minerals were redeposited in given short time frame (Fig. 3), thereby increasing the maximum concentration up to $0.015 \text{ g}\cdot\text{l}^{-1}$ at a 15 cm distance from the inlet. As observed in the experiment, insignificant amounts of reducer were leached, and pushed further away from the inlet. Oxidized reductant can clearly be seen through the glass box in the laboratory experiment as well as in the results of the numerical experiments (Fig. 3).

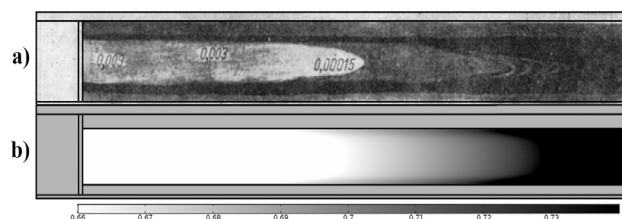


Fig. 3. Results of the numerical simulation compared to laboratory experiment: (a) experimental results showing the observed concentration along the box [12]; (b) dissolution of the reducer inside the box as obtained by numerical simulation.

The numerical simulation results were achieved, and began to fit the experimental data (Fig. 4) when the reduction reactions rate were significantly higher than the oxidation reactions rate, meaning that the concentration of reducer is higher than the concentration of oxidant.

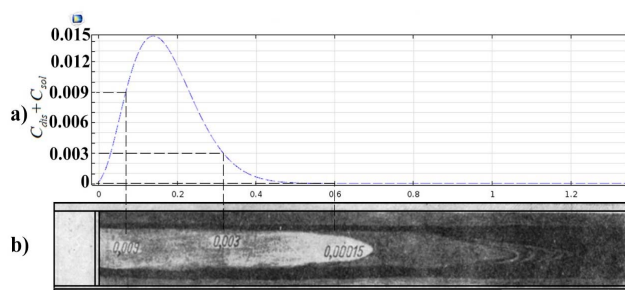


Fig. 4. Total concentration of uranium (solid and dissolved) (in $\text{g}\cdot\text{l}^{-1}$) against distance (in m) from the inlet of the box calculated by numerical simulation as compared to the laboratory experiment.

Upon conforming with the laboratory experiment, numerical simulation was further extended while crescent shaped rollfront redistributed concentrations were observed in the numerical simulation as illustrated on Fig. 4 over a period of 3.300 days with an inflow velocity at $10^{-4} \text{ m}\cdot\text{s}^{-1}$; in these conditions, the deposit moved over a distance of about 15 m conserving its shape.

The rollfront is gradually shifted over time along the stream flow (Fig. 5), despite of the absence of the convection or diffusion terms in the solid uranium concentration equation. Hence, this shift is a result of the dissolution/precipitation chemical reactions. The reducer is leached and redeposited together with the uranium minerals while some of its concentration is consumed in order to reduce the dissolved uranium.

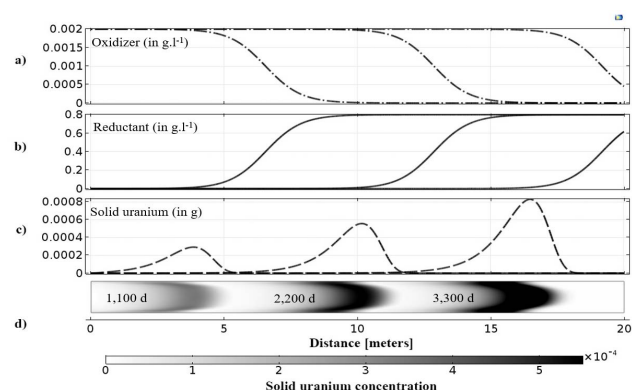


Fig. 5. Re-deposition of uranium over the periods of 1.100, 2.200, and 3.300 days: (a) oxidizer concentration; (b) reductant concentration; (c) solid uranium concentration; (d) solid uranium concentration in 2D.

One should note that a small hose is observed in the velocity field near the inflow point both in the laboratory and in the numerical experiment. The non-parallel flow at the inlet is probably at the origin of the crescent shape observed in the uranium deposition (Fig. 6), the flow being higher in the middle of the box than on the edges (no uniform inlet flow). Then, the flow stabilizes into a parallel flow regime for greater distances, indicating that this is not the viscosity of the fluid which is at the origin of the slowdown of the flow along the inlet edges.

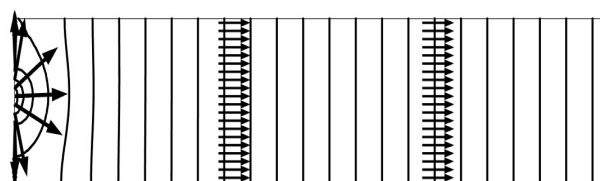


Fig. 6. Velocity field at the inlet and along the box.

To test this assumption, the boundary conditions were redesigned without this narrowing in the inflow. The recalculation gives a results with a straight front (Fig. 7). Therefore, the rollfront shape would result in a non-homogeneously distributed inlet velocity flow.

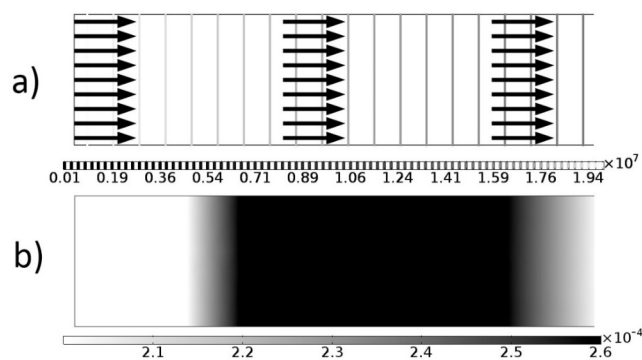


Fig. 7. Numerical results for unconstructed non-expanding channel: (a) velocity (shown as arrows) and pressure (shown via vertical lines) distribution; (b) shape of a rollfront deposit in 2D vertical section.

Therefore, these numerical tests suggest that it that the roll-like shapes forms due to a squeeze (or constriction) of the channel in which the flow occurs, and consequently increase the flow velocity, and thus to a subsequent change in the pressure gradient. Further numerical experiments were conducted with various channel constrictions (Fig. 8).

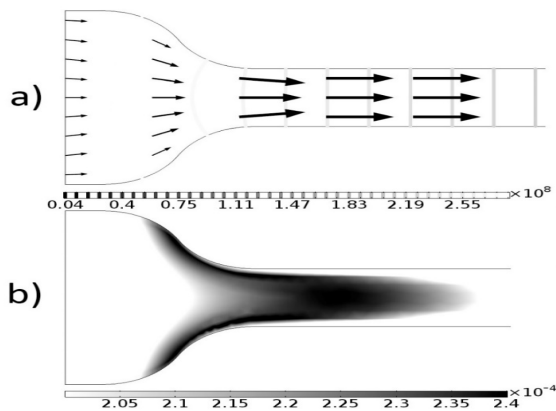


Fig. 8. Resulting solid mineral concentration with the typical crescent like shape for the rollfront. Lines represent flow velocity.

Various geometries with widening (Fig. 9), and constricting and expanding channels (Fig. 10), were numerically simulated both for the pressure field, and for the solid mineral concentration. All these cases exhibit a crescent like shape front. Even after the pressure distribution straightens, the concentration front does not recover its original shape. This can be explained by the fact that in the experiment, the concentration of oxygen probably was too low to redeposit substantial amounts of mineral further to the right during such a short period.

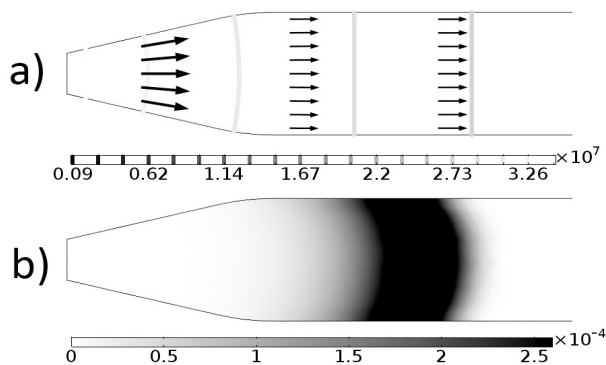


Fig. 9. Crescent shape resulting from expansion of the channel.

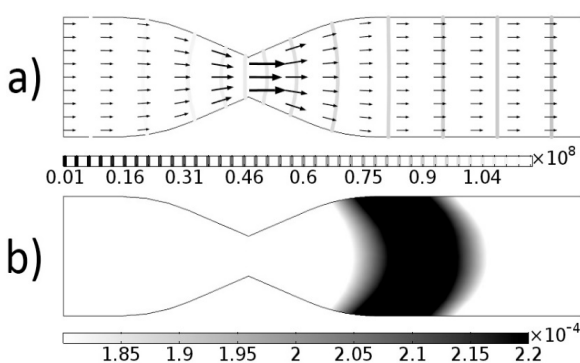


Fig. 10. Crescent shaped rollfront after constriction and expansion of the channel.

Dissolved uranium can “slip through” a reductant zone and precipitate somewhere further downstream [15]. These conditions were also numerically simulated by adding two zones with reductant (Fig. 11). In this case, two rollfronts can occur in the same channel at the same time. Once concentration of reductant at upstream zone is depleted, mineral will migrate into downstream reductant zone.

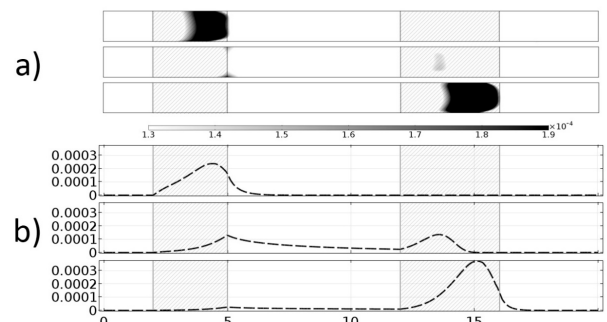


Fig. 11. Uranium concentration slipping through one reducing zone to another: (a) 2D solid uranium concentration; (b) solid uranium concentration in 1D.

According to the conducted numerical simulations, the rollfront moving velocity depends linearly on the groundwater flow velocity on a log-log plot (Fig. 12). Likewise, linear velocity was observed for different reductant concentrations as shown on Fig. 13 thus, the velocity ratio of the rollfront moving velocity over the groundwater flow velocity is most likely constant. For instance, at oxidant concentration equal to $0.02 \text{ g}\cdot\text{l}^{-1}$ and reductant concentration equal to $0.8 \text{ g}\cdot\text{l}^{-1}$, the rollfront re-deposition velocity was 240 times slower compared to the groundwater flow velocity (Fig. 12).

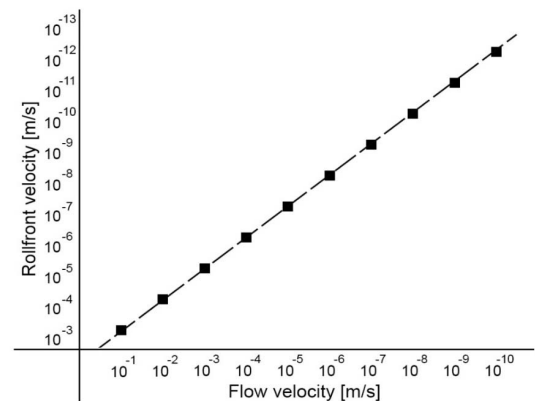


Fig. 12. Flow velocity of groundwater versus rollfront velocity at reductant concentration $0.8 \text{ g}\cdot\text{l}^{-1}$ and oxidant concentration $0.02 \text{ g}\cdot\text{l}^{-1}$. Both axes are in logarithmic scale.

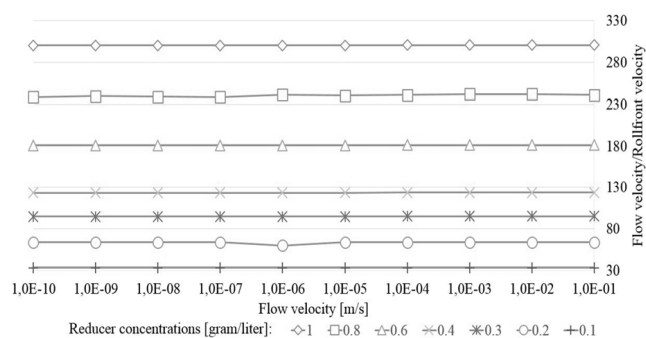


Fig. 13. Dependence between ratio of rollfront velocity over flow velocity and reducer concentration.

The rollfront deposits in Chu-Sarysu basin (Kazakhstan) is at the distance of 600 km from the assumed leached uranium source located in the Tianshan Mountains. In other words, the dissolved uranium brine flowed in the unconsolidated sands to its current location over a distance of about 600 km [3].

According to Brovin et al. [15], the average filtration velocity of the groundwater is 0.8–1.3 m.yr⁻¹ meters per year [about 2.5–4.4 10⁻⁸ m.s⁻¹]. Given these groundwater flow velocities range, it would take about from 111 to 180 million years for the rollfront to cover this distance, assuming that highly reducing environment and oxidant are preserved. The rise of Tianshan mountains and consequently the event which caused the leaching and the deposition of the uranium in the Chu-Sarysu basin happened approximately 23–33 million years ago [3], which suggests that average initial concentration of reducing agents along the stream path had to be equal to approximately 0.16 gram per liter.

4. Conclusions

The roll shaped formations in sandstone uranium deposits evidently occur due to a change in the geometry of the permeable formations. Numerical results show that both constriction and expansion of the permeable channels result in crescent shaped deposits.

Convection and reactions during uranium precipitation and dissolution were main mechanisms of rollfront formation. Convection is influenced by the pressure difference due to geological inclination, geometry and filtration properties of the channels. Reactions depend on properties of particular chemical complexes involved in the formation of rollfront. One of the major pitfalls in current modeling of the rollfront deposits can form from the

reactive transport standpoint, and lay in the unknown rate of the reaction coefficients between the solutions containing the dissolved mineral and the reducing environment. Most likely, this is an important point that implies that these parameters are subject for adjustment for a specific deposit after an appropriate laboratory experimentation. Apparently, the rate of the reaction by itself dictates the spreading length of the solid mineral along the streamlines. Other factors that control the distances at which the minerals migrate in reduced sandstones include the reductant and dissolved mineral concentrations. A deficit in any of these parameters decrease the spreading of the uranium precipitation, thereby lengthening the migration distance of a mineral before it crystallizes.

Assuming a linear dependence of flow velocity and rollfront velocity as observed in the numerical experiments, it might be possible to predict reducer concentrations, or in large scale determine probable locations of rollfront deposits.

Model can potentially be used to generate synthetic data for deposits formed via infiltration of minerals through porous medium and redox chemical reactions, to test and verify any prospective modeling techniques based non-deterministic approaches. Furthermore, the model can be further applied to enhance existing stochastic modeling methods by providing additional input data based on the results of reactive transport simulation.

Acknowledgements

The work was partially supported by the Ministry of Education and Science of Kazakhstan through grant financing project GF4/3290 and program of targeted financing BR05236447.

References

- [1]. S.S. Adams, R.T. Cramer. Data-process-criteria model for roll-type uranium deposits. Geological environments of sandstone-type uranium deposits. Report IAEA-TECDOC-328. International Atomic Energy Agency, Vienna (Austria); p. 408; Mar 1985; p. 383–399.
- [2]. World Distribution of Uranium Deposits (UDEPO) with Uranium Deposit Classification, IAEA-TECDOC-1629, International Atomic Energy Agency, Printed by the IAEA in Austria October 2009, p. 117. ISBN 978–92–0–110509–7
- [3]. F.J. Dahlkamp. Uranium Deposits of the World (Asia), Springer-Verlag, Berlin Heidelberg, 2009, p. 492

- [4]. A Joint Report by the OECD Nuclear Energy Agency and the International Atomic Energy Agency "Uranium 2014: Resources, Production and Demand", Organisation for Economic Co-operation and Development, 2014, NEA No. 7209.
- [5]. A.B. Tarkhanov, Y.P. Bugrieva. Large uranium deposits of the world. *Mineral'noe syr'e* [Minerals Journal] 27 (2012) 118 p. (in Russian).
- [6]. D. Renard, H. Beucher, *Applied Earth Science. Transactions of the Institutions of Mining and Metallurgy: Section B* 121 (2012) 84–88. DOI: 10.1179/1743275812Y.0000000011
- [7]. G. Petit, H. Boissezon, V. Langlais, G. Rumbach, A. Khairuldin, T. Oppeneau, N. Fiet. Application of Stochastic Simulations and Quantifying Uncertainties in the Drilling of Roll Front Uranium Deposits. In: Abrahamsen P., Hauge R., Kolbjørnsen O. (eds) *Geostatistics Oslo 2012. Quantitative Geology and Geostatistics*, Springer, Dordrecht 17 (2012) 321–332. DOI 10.1007/978-94-007-4153-9_26
- [8]. M. Abzalov, S. Drobov, O. Gorbatenko, A. Vershkov, O. Bertoli, D. Renard, H. Beucher, *Applied Earth Science* (123) (2014) 70–85. DOI: 10.1179/1743275814Y.0000000055
- [9]. S.B. Romberger. Transport and deposition of uranium in hydrothermal systems at temperatures up to 300 °C: geological implications. In: De Vivo B., Ippolito F., Capaldi G., Simpson P.R. (eds.) *Uranium geochemistry, mineralogy, geology, exploration and resources*. Springer, Dordrecht 1 (1984) 12–17. DOI: 10.1007/978-94-009-6060-2_3
- [10]. M.F. Maksimova, Y.M. Shmariovich, *Plastovo-infiltratsionnoye rudoobrazovanie* [Stratum-infiltration ore formation]. Nedra, Moscow, Russia, 1993, p. 160 (in Russian).
- [11]. M. A. Goldshtik, *Processy perenosy v zernistom sloe* [Transfer processes in granular layer], Institute of Thermophysics, Novosibirsk, Russia, 1984, p. 163 (in Russian).
- [12]. L.S. Evseeva, K.E. Ivanov, V.I. Kochetkov. Some laws of the formation of epigenetic uranium ores in sandstones, derived from experimental and radiochemical data, *Atomnaya Energiya* [Atomic Energy] 14 (1962) 474–481 (in Russian).
- [13]. J. Bear, *Dynamics of Fluids in Porous Media*. American Elsevier Publishing Company, New York, 1972, 764 p.
- [14]. N.T. Danaev, N.K. Korsakova, V.I. Pen'kovskij. *Massoperenos v priskvazhinnoi zone i elektromagnitnyi karotazh plasta* [Mass transfer in the borehole zone and electromagnetic stratum well logging], Al-Farabi Kazakh National University, Kazakhstan, 2005, p. 180 (in Russian).
- [15]. K.G. Brovin, V.A. Grabovnikov, M.V. Shumilin, V.G. Yazikov. *Prognoz, poiski, razvedka i promyshlennaya ocenka mestorozhdeniy urana dlya otrabotki podzemnym vyshelachivaniyem* [Forecast, search, exploration and industrial estimation of uranium deposits for production with in-situ leaching method]. Gylym, Almaty, Kazakhstan, 1997, p. 384 (in Russian).